Archaeometry Laboratory
University of Missouri Research Reactor

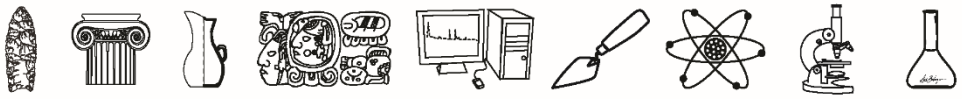

Compositional Analysis of Formative Period Ceramic and Geological Materials from Potrero Mendieta in the Jubones River Basin, Southwester Ecuador, (ca. 4400 -300 BCE)

Preliminary Ceramic Compositional Analysis

FIRST REPORT

ANIDS: MED 001-050

Prepared by:
William D. Gilstrap
Archaeometry Laboratory,
University of Missouri Research Reactor
Columbia, MO 65211
gilstrap@mit.edu

Prepared for:
Miriam E. Domínguez
Department of Anthropology
University of Florida
1112 Turlington Hall
PO Box 117305
Gainesville, FL 32611-730
Mdoming1@ufl.edu

22 February 2017

Introduction

This report summarizes the findings from the compositional analysis of 48 ceramic sherds and two geological clay samples by NAA. All material derives from the Formative Period site of Potrero Mundieta in southern Ecuador. The ceramic specimens were selected from four discrete structures – Structure 1 (n = 20), Structure 2 (n = 20), Structure 3 (n = 3); and Structure 4 (n = 3) – at differing depths of deposition. Two more ceramic samples were selected from the same vicinity as the two clay samples found on site, STP10. The ceramic material is poorly preserved and no stylistic information was retrieved. The goal of the project is to identify compositional similarities within the ceramic assemblage and to attempt to identify imported vessels through comparison with reference groups of the Ecuadorian coast and northern Andes established previously by Jamieson et al. (2013) and unpublished reference groups from R. Lippi and M. Masucci.

The resulting data analysis identified and characterized four tentative compositional groups, two loners and several unassigned samples. None of which I was able to match with any previously existing reference group from Lippi or Masucci. A number of samples, however, may be tentatively viewed as compatible with compositional groups derived from archaeological material local to Quito (Jamison et al. 2013). Compositional groups published by Jamieson et al. (2013) were produced at the reactor housed at McMaster and are not directly compatible with data produced at MURR without an inter-laboratory calibration factor and any compatibility found within the comparison made in this report should be viewed with caution.

The finalized chemical groups are subsequently compared against the petrographic study of samples MED001-020 conducted by Ann S. Cordell of the Florida Museum of Natural History.

Below you will find a description of the sample preparation and analytical techniques used at MURR and report the subgroup structure identified through quantitative analysis of the compositional dataset. This is followed by a detailed description of the data analysis and each identified group.

Sample Preparation

Specimens were prepared for INAA using procedures established at the Archaeometry Laboratory (Glascock 1992, Glascock and Neff 2003). Fragments of about 1cm^2 were removed from each sherd and abraded using a silicon carbide burr in order to remove surface treatments (e.g., glaze, slip, paint) and adhering soil, thereby reducing the risk of measuring contamination. The specimens were washed in deionized water and allowed to dry in the laboratory. Once dry, the individual sherds were ground to powder in an agate mortar to homogenize them. Archival portions were retained from each sherd (when possible) for future research.

Two analytical samples were prepared from each specimen. Portions of approximately 150 mg of powder were weighed into high-density polyethylene vials used for short irradiations at MURR. At the same time, 200 mg aliquots from each sample were weighed into high-purity quartz vials used for long irradiations. Individual sample weights were recorded to the nearest 0.01 mg using an analytical balance. Both vials were sealed prior to irradiation. Along with the unknown samples, standards made from National Institute of Standards and Technology (NIST) certified standard reference materials of SRM-1633b (coal fly ash) and SRM-688 (basalt rock) were similarly prepared, as were quality control

samples (e.g., standards treated as unknowns) of SRM-278 (obsidian rock) and Ohio Red Clay (a standard developed for in-house applications).

Irradiation and Gamma-Ray Spectroscopy

Procedures used for the irradiation and gamma-ray spectroscopy follow established MURR Archaeometry Laboratory protocol (Glascock 1992; Glascock and Neff 2003; Neff 2000). Neutron activation analysis of ceramics at MURR, which consists of two irradiations and a total of three gamma counts, constitutes a superset of the procedures used at most other NAA laboratories (Glascock 1992; Glascock and Neff 2003; Neff 2000). As discussed in detail by Glascock (1992), a short irradiation is carried out through the pneumatic tube irradiation system. Specimens in the polyvials are sequentially irradiated, two at a time, for five seconds by a neutron flux of 8×10^{13} n cm^{-2} s^{-1}. The 720-second count yields gamma spectra containing peaks for nine short-lived elements aluminum (Al), barium (Ba), calcium (Ca), dysprosium (Dy), potassium (K), manganese (Mn), sodium (Na), titanium (Ti), and vanadium (V). The specimens are encapsulated in quartz vials and are subjected to a 24-hour irradiation at a neutron flux of 5×10^{13} n cm^{-2} s^{-1}. This long irradiation is analogous to the single irradiation utilized at most other laboratories. After the long irradiation, specimens decay for seven days, and then are counted for 1800 seconds (the "middle count") on a high-resolution germanium detector coupled to an automatic sample changer. The middle count yields determinations of seven medium half-life elements, namely arsenic (As), lanthanum (La), lutetium (Lu), neodymium (Nd), samarium (Sm), uranium (U), and ytterbium (Yb). After an additional three- or four-week decay, a final count of 8500 seconds is carried out on each specimen. The latter measurement yields the following 17 long half-life elements: cerium (Ce), cobalt (Co), chromium (Cr), cesium (Cs), europium (Eu), iron (Fe), hafnium (Hf), nickel (Ni), rubidium (Rb), antimony (Sb), scandium (Sc), strontium (Sr), tantalum (Ta), terbium (Tb), thorium (Th), zinc (Zn), and zirconium (Zr).

The element concentration data from the three measurements were tabulated in parts per million using Microsoft® Office Excel. Descriptive and contextual information for the specimen were appended to the spreadsheet of elemental abundances. These data are provided as an appendix to this report and as an accompanying digital file. Additional copies of these data are available upon request to the MURR Archaeometry Laboratory. Following our Data Management and Sharing Plan (Boulanger and Stoner 2012) these data will be made available via our data-sharing portal within a period of not less than two years from the issuance of this report.

Interpreting Chemical Data

Analyses at MURR typically produce elemental concentration values for 33–34 elements. Some elements are present at or below the detection limits for neutron activation using our current procedures. If greater than 50% of specimens are missing values for a particular element, this element is removed from consideration in the analysis. Statistical analyses are carried out on base-10 logarithms of elemental concentrations. Use of log concentrations rather than raw data compensates for differences in magnitude between the major elements, such as Na, and trace elements, such as the rare earth or lanthanide elements (REEs). Transformation to base-10 logarithms also yields a more normal distribution for many trace elements.

The interpretation of compositional data obtained from the analysis of archaeological materials is discussed in detail elsewhere (e.g., Baxter and Buck 2000; Bieber, et al. 1976; Bishop and Neff 1989; Glascock 1992; Harbottle 1976; Neff 2000) and will only be summarized here. The main goal of data

analysis is to identify distinct homogeneous groups within the analytical database. Based on the provenance postulate of Weigand et al. (1977), different chemical groups may be assumed to represent geographically restricted sources. For lithic materials such as obsidian, basalt, and cryptocrystalline silicates (e.g., chert, flint, or jasper), raw material samples are frequently collected from known outcrops or secondary deposits and the compositional data obtained on the samples is used to define the source localities or boundaries. The locations of sources can also be inferred by comparing unknown specimens (i.e., ceramic artifacts) to knowns (i.e., clay samples) or by indirect methods such as the "criterion of abundance" (Bishop, et al. 1982) or by arguments based on geological and sedimentological characteristics (e.g., Steponaitis, et al. 1996). The ubiquity of ceramic raw materials usually makes it impossible to sample all potential "sources" intensively enough to create groups of knowns to which unknowns can be compared. Lithic sources tend to be more localized and compositionally homogeneous in the case of obsidian or compositionally heterogeneous as is the case for most cherts.

Compositional groups can be viewed as "centers of mass" in the compositional hyperspace described by the measured elemental data. Groups are characterized by the locations of their centroids and the unique relationships (i.e., correlations) between the elements. Decisions about whether to assign a specimen to a particular compositional group are based on the overall probability that the measured concentrations for the specimen could have been obtained from that group.

Initial hypotheses about source-related subgroups in the compositional data can be derived from non-compositional information (e.g., archaeological context, decorative attributes) or from application of various pattern-recognition techniques to multivariate chemical data. Some pattern recognition techniques used to investigate archaeological datasets are cluster analysis (CA), principal components analysis (PCA), and discriminant analysis (DA). Each of the techniques has its own advantages and disadvantages which may depend upon the types and quantity of data available for interpretation.

The variables (measured elements) in archaeological and geological datasets are often correlated and frequently large in number. This makes handling and interpreting patterns within the data difficult. Therefore, it is often useful to transform the original variables into a smaller set of uncorrelated variables in order to make data interpretation easier. Of the above-mentioned pattern recognition techniques, PCA is a technique that transforms from the data from the original correlated variables into uncorrelated variables most easily.

Principal components analysis creates a new set of reference axes arranged in decreasing order of variance subsumed. The individual PCs are linear combinations of the original variables. The data can be displayed on combinations of the new axes, just as they can be displayed on the original elemental concentration axes. PCA can be used in a pure pattern-recognition mode, e.g., to search for subgroups in an undifferentiated data set, or in a more evaluative mode, e.g., to assess the coherence of hypothetical groups suggested by other criteria. Generally, compositional differences between specimens can be expected to be larger for specimens in different groups than for specimens in the same group, and this implies that groups should be detectable as distinct areas of high point density on plots of the first few components.

Principal components analysis of chemical data is scale dependent, and analyses tend to be dominated by those elements or isotopes for which the concentrations are relatively large. As a result, standardization methods are common to most statistical packages. A common approach is to transform

the data into logarithms (e.g., base 10). As an initial step in the PCA of most chemical data at MURR, the data are transformed into log concentrations to equalize the differences in variance between the major elements such as Al, Ca and Fe, on one hand and trace elements, such as the rare-earth elements (REEs), on the other hand. An additional advantage of the transformation is that it appears to produce more nearly normal distributions for the trace elements.

One frequently exploited strength of PCA, discussed by Baxter (1992), Baxter and Buck (2000), and Neff (1994; 2002), is that it can be applied as a simultaneous R- and Q-mode technique, with both variables (elements) and objects (individual analyzed samples) displayed on the same set of principal component reference axes. A plot using the first two principal components as axes is usually the best possible two-dimensional representation of the correlation or variance-covariance structure within the data set. Small angles between the vectors from the origin to variable coordinates indicate strong positive correlation; angles at 90 degrees indicate no correlation; and angles close to 180 degrees indicate strong negative correlation. Likewise, a plot of sample coordinates on these same axes will be the best two-dimensional representation of Euclidean relations among the samples in log-concentration space (if the PCA was based on the variance-covariance matrix) or standardized log-concentration space (if the PCA was based on the correlation matrix). Displaying both objects and variables on the same plot makes it possible to observe the contributions of specific elements to group separation and to the distinctive shapes of the various groups. Such a plot is commonly referred to as a *biplot* in reference to the simultaneous plotting of objects and variables. The variable inter-relationships inferred from a biplot can be verified directly by inspecting bivariate elemental concentration plots.

Whether a group can be discriminated easily from other groups can be evaluated visually in two dimensions or statistically in multiple dimensions. A metric known as the Mahalanobis distance (or generalized distance) makes it possible to describe the separation between groups or between individual samples and groups on multiple dimensions. The Mahalanobis distance of a specimen from a group centroid (Bieber et al. 1976; Bishop and Neff 1989) is defined by:

$$D^2_{y,x} = [y - \bar{X}]^t \, I_x \, [y - \bar{X}]$$

where y is the $1 \times m$ array of logged elemental concentrations for the specimen of interest, x is the $n \times m$ data matrix of logged concentrations for the group to which the point is being compared with $\bar{X}$ being it $1 \times m$ centroid, and I_x is the inverse of the $m \times m$ variance–covariance matrix of group x. Because Mahalanobis distance takes into account variances and covariances in the multivariate group it is analogous to expressing distance from a univariate mean in standard deviation units. Like standard deviation units, Mahalanobis distances can be converted into probabilities of group membership for individual specimens. For relatively small sample sizes, it is appropriate to base probabilities on Hotelling's T^2, which is the multivariate extension of the univariate Student's t.

When group sizes are small, Mahalanobis distance-based probabilities can fluctuate dramatically depending upon whether or not each specimen is assumed to be a member of the group to which it is being compared. Harbottle (1976) calls this phenomenon *stretchability* in reference to the tendency of an included specimen to stretch the group in the direction of its own location in elemental concentration space. This problem can be circumvented by cross-validation, that is, by removing each specimen from its presumed group before calculating its own probability of membership (Baxter 1994; Leese and Main 1994). This is a conservative approach to group evaluation that may sometimes exclude true group members.

Small sample and group sizes place further constraints on the use of Mahalanobis distance: with more elements than samples, the group variance-covariance matrix is singular thus rendering calculation of I_x (and D^2 itself) impossible. Therefore, the dimensionality of the groups must somehow be reduced. One approach would be to eliminate elements considered irrelevant or redundant. The problem with this approach is that the investigator's preconceptions about which elements should be discriminate may not be valid. It also squanders the main advantage of multielement analysis, namely the capability to measure a large number of elements. An alternative approach is to calculate Mahalanobis distances with the scores on principal components extracted from the variance-covariance or correlation matrix for the complete data set. This approach entails only the assumption, entirely reasonable in light of the above discussion of PCA, that most group-separating differences should be visible on the first several PCs. Unless a data set is extremely complex, containing numerous distinct groups, using enough components to subsume at least 90% of the total variance in the data can be generally assumed to yield Mahalanobis distances that approximate Mahalanobis distances in full elemental concentration space.

Lastly, Mahalanobis distance calculations are also quite useful for handling missing data (Sayre 1975). When many specimens are analyzed for a large number of elements, it is almost certain that a few element concentrations will be missed for some of the specimens. This occurs most frequently when the concentration for an element is near the detection limit. Rather than eliminate the specimen or the element from consideration, it is possible to substitute a missing value by replacing it with a value that minimizes the Mahalanobis distance for the specimen from the group centroid. Thus, those few specimens which are missing a single concentration value can still be used in group calculations.

Results

Before any statistical analysis could be performed it was necessary to remove the element Nickel (Ni) from the entire dataset as the majority of samples registered values lower than the limits of detection in our laboratory. Two other elements, arsenic (As) and antimony (Sb), an element often associated with As, were removed due to their high degrees of solubility in soils and potential for contamination of ceramic material during post-depositional phases. The removal of these elements is a preventative measure to avoid any potential skewing of the data during the statistical investigations have been removed from the dataset.

With the removal of As, Ni and Sb, the dataset was evaluated for the total variation of each element by calculating a total variation matrix (Aichenson 1986; Buxeda i Garrigós1999; Buxeda i Garrigós et al. 2001; Buxeda i Garrigós and Kilikoglou 2003; Kilikoglou et al. 2007). A total variation matrix (TVM) is constructed of a table composed of log-transformed data where each element is expressed as a ratio of all other elements in the dataset (See Appendix II). Examination of the TVM has provided several pieces of key information for subsequent sample grouping and overall archaeological interpretation of the dataset. One of the main functions of the TVM is to demonstrate which variables (elements) have the most or least amount of variation within a dataset. In this case, the transition metal chromium (Cr) shows the most variation while aluminum (Al), a transition metal and major component of clays and soils, has the least amount of variation in the dataset. Chromium is an element that is often used to discriminate compositional groups in ceramic studies as it can relate to very specific geological components.

Second, the TVM has calculated a total variation (*vt*) value of 3.911. Total variation is the sum of all variances in the variation matrix divided by twice the number of elements in the matrix (Buxeda i

Garrigós and Kilikoglou 2003:186). This value provides a metric to evaluate variability in a chemical dataset which is compatible with both variances and Euclidean distances (Schwalbe and Cuthbert 1988). This value is significant to the evaluation of ceramic composition studies as it is an indicator of what is referred to as monogenic or polygenic datasets. A low value indicates a monogenic dataset. For a study of ceramic composition, this translates to a group made from chemically indiscrete raw materials (a group from a single origin). Polygenic datasets suggest that there is more than one discernable composition group in the dataset. Often the integer is equivalent to the amount of groups present in a single dataset, i.e. a *vt* value of 3.045 suggests that there are at least three compositionally discrete groups present in a dataset. The high *vt* value of 3.911 suggests that this dataset is polygenic and consists of multiple groups deriving from either discrete geological source materials or different production practices that result in altered chemical compositions (i.e. clay mixing, use of temper, etc.).

With the removal of these problematic elements, the dataset was subjected to a Principal Component Analysis (PCA). This test demonstrated that greater than 91% of the cumulative variance can be explained by the first eight principal components (Table 1). Principal component (PC) 1 is only slightly positively loaded on the alkali elements K and Rb and the rare-earth element U. PC 1 has heavy negative loading on several elements including Mn, Ca and Zn. The second component, PC 2 is positively loaded on Cr, showing consistency with the TVM above, and negatively loaded on Na. A biplot of these first two PCs displays the general structure of the dataset while accounting for over 56% of the cumulative variance (Figure 1). The structure illustrated by Figure 1 suggests that there are a upwards of four compositional groups with several outliers that can be discriminated from the original dataset. This result is consistent with the results of the TVM described above indicating that he dataset is indeed polygenic. The resulting groups are described immediately below.

Group 1(DOM-1) is consists of the majority of samples from the MED assemblage with 26 group members. DOM-1 is characterized mainly by elevated levels of Ca and Mn (Figure 2), and elevated levels of actinide elements (REEs). Groups DOM-2 (n = 4) and DOM-2A (n= 2) have comparatively elevated concentrations of alkali elements: K, Rb and Cs (Figure 3) in addition to higher concentrations of U and Th. Group DOM-3 is set apart from all other samples with very high levels of Cr. Sample MED017 was separated as a loner due to elevated Na and low Cr concentration values. Sample MED 020 was also separated out due to very low Na and Ca concentrations.

Twelve ceramic samples and both clay samples were left unassigned (DOM-UNK). These samples vary in chemical composition and could not be grouped together or with any of the aforementioned compositional groups. Samples from all four structures are left in this group. It is notable that MED017 exhibits a completely different chemical signature than all other samples in the MED dataset. MED035, and MED039 often plot within the confidence ellipse of DOM-1 (Figure 3), but do not meet the 1% group membership probability cutoff (Table 2). MED015 and MED016 show 2% and 18% group membership probabilities but have been kept separate from DOM-1 due to differences in several elements; they are considered associated members.

All of the established groups and unassigned samples were tested against all groups identified in the unpublished study by Lippi and by Masucci and against the study of Jamison et al (2013) with no clear matches. Additionally, no compositional group matched either of the locally sampled clays submitted for comparison.

Comparison with petrographic data

Samples MED001-020 were selected for additional petrographic analysis carried out by Ann Cordell at the Florida Museum of Natural History. Petrographic results indicate that there are at three different ceramic fabrics as determined by the felsic, mafic and volcanic nature of the inclusions (called "temper" in Cordell's study). The majority of the samples in the Mafic and Felsic petro-groups were assigned to chemical group DOM-1 with the exception MED002, MED016 and MED018, Both MED002 and MED018 were assigned to chemical group DOM-2. While MED 016 has been identified as an associated member of DOM-1.

The chemical link between the Felsic and Mafic petro-groups is likely due to the heterogeneity of the samples themselves. The descriptions of the groups show a grading of rock material from felsic to intermediate (probably dependent on the occurrence of ferromagnesian minerals biotite and hornblende amphibole) and intermediate to felsic (probably dependent on the occurrence of biotite, hornblende and the lack of quartz and/or alkali feldspars). Both petrofabrics appear to consist of, at least partially, intermediate igneous plutonic rock fragments such as granodiorite. Perhaps the variation seen in the relatively small fragments in the vessels are variants of the same intermediate rock formation. This statement is only a hypothesis and must be investigated further. There is evidence for geological outcrops of all petrographically identified materials present in the ceramic fabrics (Longo and Baldock 1982) and it may be likely that the potters of this region are collecting rocks that look similar from these different outcrops to use as tempering materials as suggested by Cordell. It may be that these rocks are difficult to distinguish chemically as they are composed of similar mineralogical suites.

Discussion and conclusions

The results of the chemical study in comparison with the petrographic study seem to suggest that the majority of pottery are made using locally available raw materials such as volcanoclastic rock, granite and granodiorite as temper. Although neither clay submitted for analysis were a chemical match for any of the resulting chemical groups, Cordell's petrographic study seems to suggest that they could have been used for production due to similarities in the presence/absence of siliceous microfossils. The results are still inconclusive. In terms of chemistry alone, it may be that the clays without the rock temper added to the clay, the ceramic fabric may have a significantly different chemical signature.

Looking at the chemistry of the larger assemblage, it seems likely that compositional groups DOM-2, DOM-2A and DOM-3 are composed of different raw materials than DOM-1. DOM-2 contains two samples from the Felsic group of the petrographic study, MED002 and MED018. It seems that when compared against a greater number of samples, these two sherds were more readily distinguishable from the main group. As these samples are granitic in nature, they may have been produced from a combination of mineralogically similar, but chemically different raw materials. DOM-2A and DOM-3 are, chemically speaking, very different from DOM-1 and likely represent material brought in from elsewhere. Unfortunately none of the samples that make up these chemical groups were present in the petrographic study.

Acknowledgments

Daniel Lee was responsible for preparation and irradiation of all project specimens. This project was supported in part by NSF grant BCS- 1415403 to the Archaeometry Laboratory of the Research

Reactor, University of Missouri.

References

Aichenson, J.
1986 *The Statistical Analysis of Compositional Data.* Monographs on Statistics and Applied Probability. Chapman and Hall, Ney York.

Arnold, D.E.
1985 *Ceramic theory and cultural process*. Cambridge University Press, Cambridge.

Baxter, M. J.
1992 Archaeological Uses of the Biplot—A Neglected Technique? In *Computer Applications and Quantitative Methods in Archaeology, 1991*, edited by G. Lock and J. Moffett, pp. 141-148. BAR International Series. vol. S577. Tempvs Reparatvm, Oxford.

1994 *Exploratory Multivariate Analysis in Archaeology*. Edinburgh University Press, Edinburgh.

Baxter, M. J. and C. E. Buck
2000 Data Handling and Statistical Analysis. In *Modern Analytical Methods in Art and Archaeology*, edited by E. Ciliberto and G. Spoto, pp. 681-746. John Wiley and Sons, New York.

Boulanger, M.T. and W.D. Stoner
2012 Data Management and Sharing Plan (v. 1). Electronic document available at: http://archaeometry.missouri.edu/data_management_policy.html. Last updated: August 2012. Accessed on: December 28, 2012.

Bieber, A. M. J., D. W. Brooks, G. Harbottle and E. V. Sayre
1976 Application of Multivariate Techniques to Analytical Data on Aegean Ceramics. *Archaeometry* 18:59-74.

Bishop, R. L. and H. Neff
1989 Compositional Data Analysis in Archaeology. In *Archaeological Chemistry IV*, edited by R. O. Allen, pp. 576-586. Advances in Chemistry. vol. 220. American Chemical Society, Washington, D.C.

Bishop, R. L., R. L. Rands and G. R. Holley
1982 Ceramic Compositional Analysis in Archaeological Perspective. *Advances in Archaeological Method and Theory* 5:275-330.

Buxeda i Garrigós, J.
1999 Alteration and Contamination of Archaeological Ceramics: The Perturbation Problem. *Journal of Archaeological Science* 26:295-313.

Buxeda i Garrigós, J., Cau Ontiveros, M. A. and V. Kilikoglou
2003 Chemical variability in Clays and Pottery from a Traditional Cooking Pot Village: Testing Assumptions in Pereruela. *Archaeometry* 45:1-17.

Buxeda i Garrigós, J. and V. Kilikoglou
2003 Total Variation as a Measure of Variability in Chemical Datasets. In *Patterns and Process, a Festschrist in Honor of Dr. Edward V. Sayre*, edited by L. Van Zelst. pp. 185-198. Smithsonian Center for Materials Research and Education: Washington D.C.

Buxeda i Garrigós, J., Kilikoglou, V. and P. M. Day
2001 Chemical and Mineralogical Alteration of Ceramics from a Late Bronze Age Kiln at Kommos, Crete: The Effect on the Formation of a Reference Group. *Archaeometry* 43:349-371.

Glascock, M. D.
1992 Characterization of Archaeological Ceramics at MURR by Neutron Activation Analysis and Multivariate Statistics. In *Chemical Characterization of Ceramic Pastes in Archaeology*, edited by H. Neff, pp. 11-26. Prehistory Press, Madison, WI.

Glascock, M. D. and H. Neff
2003 Neutron Activation Analysis and Provenance Research in Archaeology. *Measurement Science and Technology* 14:1516-1526.

Harbottle, G.
1976 Activation Analysis in Archaeology. *Radiochemistry* 3(1):33-72.

Jamieson, R. W., R.G.V. Hancock, L. A. Beckwith and A. E. Pidruczny
2013 Neutron Activation Analysis of Inca and Colonial Ceramic from Central Highland Ecuador. *Archaeometry* 55(2):198-213.

Kilikoglou, V., Grimanis, A. P., Tsolakidou, A., Hein, A., Malamidou, D. and Z. Tsirtsoni
2007 Neutron Activation Patterning of Archaeological Materials at the National center for Scientific Research 'Demokritos': The Case of Black on red Neolithic Pottery from Macedonia, Greece. *Archaeometry* 49:301-319.

Leese, M. N. and P. L. Main
1994 The Efficient Computation of Unbiased Mahalanobis Distances and their Interpretation in Archaeometry. *Archaeometry* 36:307-316.

Longo, R. and J. Baldock
1982 *Nationa Geolical Map of the Republic of Ecuador*. 1:1,000,000. Minsterio de Recursos Naturales y Energeticos, Ecuador.

Masucci, M. and A. Macfarlane
1997 An Application of Geoloical Survey and Ceramic Petrology to Porvenance Studies of Guangala Phase Ceramics of Ancient Ecuador. *Geoarchaeology* 12(7):765-793.

Neff, H.
1994 RQ-mode Principal Component Analysis of Ceramic Compositional Data. *Archaeometry* 36:115-130.

2000 Neutron Activation Analysis for Provenance Determination in Archaeology. In *Modern Analytical Methods in Art and Archaeology*, edited by E. Ciliberto and G. Spoto, pp. 81-134. John Wiley and Sons, New York.

2002 Quantitative Techniques for Analyzing Ceramic Compositional Data. In *Ceramic Source Determination in the Greater Southwest*, edited by D. M. Glowacki and H. Neff. Monograph 44. Cotsen Institute of Archaeology, Los Angeles.

Neff, H., R. L. Bishop, and E. V. Sayre
1988 A Simulation Approach to the Problem of Tempering in Compositional Studies of Archaeological Ceramics. *Journal of Archaeological Science* 15: 159-172.

1989 More Observations on the Problem of Tempering in Compositional Studies of Archaeological Ceramics. *Journal of Archaeological Science* 16: 57-69.

Rice, P. M.
1987 *Pottery Analysis: A Sourcebook*. University of Chicago Press, Chicago.

Salberg, D.J., M.D. Glascock and J.R. Ferguson
2010 *Instrumental Neutron Activation Ananalysis of Ceramics from the Han River region of South Korea* (Unpublished report). Missouri University Research Reactor.

Sayre, E. V.
1975 *Brookhaven Procedures for Statistical Analyses of Multivariate Archaeometric Data*. Brookhaven National Laboratory Report BNL-23128.

Steponaitis, V., M. J. Blackman and H. Neff
1996 Large-scale Compositional Patterns in the Chemical Composition of Mississippian Pottery. *American Antiquity* 61(3):555-572.

Weigand, P. C., G. Harbottle and E. V. Sayre
1977 Turquoise Sources and Source Analysis: Mesoamerica and the Southwestern U.S.A. In *Exchange Systems in Prehistory*, edited by T. K. Earle and J. E. Ericson, pp. 15-34. Academic Press, New York.

Appendix I Tables and Figures

Table 1: Principal component analysis of the Protrero Mundieta ceramic assemblage. The first eight PCs are shown accounting for more than 91% of the cumulative variance in the dataset. Strong elemental loading of individual components values are shown in bold.

Variable	PC1	PC2	PC3	PC4	PC5	PC6	PC7	PC8
% Var.	38.27	18.44	12.01	7.03	5.73	4.02	3.32	2.43
Cum. % Var.	38.27	56.71	68.72	75.75	81.48	85.50	88.82	91.25
Eigenvalues:	0.531	0.256	0.167	0.098	0.080	0.056	0.046	0.034
K	**0.139**	0.083	0.049	**0.274**	0.221	0.134	-0.161	-0.013
Rb	**0.137**	0.116	0.128	0.168	0.081	0.266	-0.185	-0.098
U	**0.115**	**0.242**	-0.076	0.176	0.226	-0.012	0.322	-0.138
Th	0.093	**0.201**	0.043	0.092	0.068	0.054	0.126	-0.237
Cs	0.084	-0.001	**0.233**	-0.011	-0.311	0.393	-0.109	-0.143
Hf	0.072	0.068	0.079	0.063	0.075	0.007	0.103	-0.189
Ta	0.065	0.102	0.061	0.024	-0.018	0.057	0.113	-0.058
Zr	0.054	0.098	0.077	0.039	0.130	-0.036	0.102	-0.236
Zr	0.054	0.098	0.077	0.039	0.130	-0.036	0.102	-0.236
Na	0.045	**-0.214**	-0.171	0.167	0.039	0.010	-0.348	0.035
Ba	-0.029	0.080	0.005	**0.301**	-0.183	0.345	0.246	0.384
Al	-0.034	-0.024	-0.040	0.053	-0.005	0.024	0.013	0.167
Lu	-0.062	0.076	0.212	0.164	-0.046	-0.213	-0.166	-0.064
Ti	-0.067	-0.022	0.057	-0.089	-0.024	0.076	0.163	-0.072
Cr	-0.070	**0.505**	**-0.258**	**-0.237**	0.119	0.012	-0.221	0.110
Fe	-0.078	0.001	0.066	-0.136	-0.054	0.143	-0.005	-0.018
Ce	-0.083	0.172	0.020	0.170	-0.043	-0.061	0.085	-0.006
La	-0.084	0.177	-0.022	**0.209**	-0.084	-0.042	0.051	-0.023
Yb	-0.097	0.075	0.161	0.170	-0.060	-0.262	-0.114	-0.067
V	-0.108	0.008	0.058	-0.147	-0.013	0.152	0.040	-0.117
Dy	-0.147	0.042	0.123	0.194	-0.060	-0.216	-0.052	0.041
Sm	-0.149	0.113	0.041	**0.200**	-0.084	-0.150	0.021	0.023
Nd	-0.150	0.175	0.013	0.117	-0.110	-0.151	0.230	0.057
Sc	-0.170	0.055	0.094	-0.051	-0.132	-0.027	-0.120	-0.035
Co	-0.172	0.000	0.108	-0.088	0.045	0.119	0.008	-0.182
Sr	-0.179	-0.093	**-0.391**	0.193	0.014	0.171	0.159	-0.059
Eu	-0.179	0.058	-0.044	0.198	-0.059	-0.117	0.038	0.039
Tb	-0.187	0.063	0.147	0.151	-0.178	-0.166	-0.137	-0.118
Zn	**-0.209**	0.126	0.038	0.051	-0.224	0.208	-0.092	0.088
Ca	**-0.281**	-0.096	**-0.198**	0.042	0.046	0.022	-0.107	-0.354
Mn	**-0.340**	-0.093	0.246	-0.005	0.452	0.077	0.016	0.218

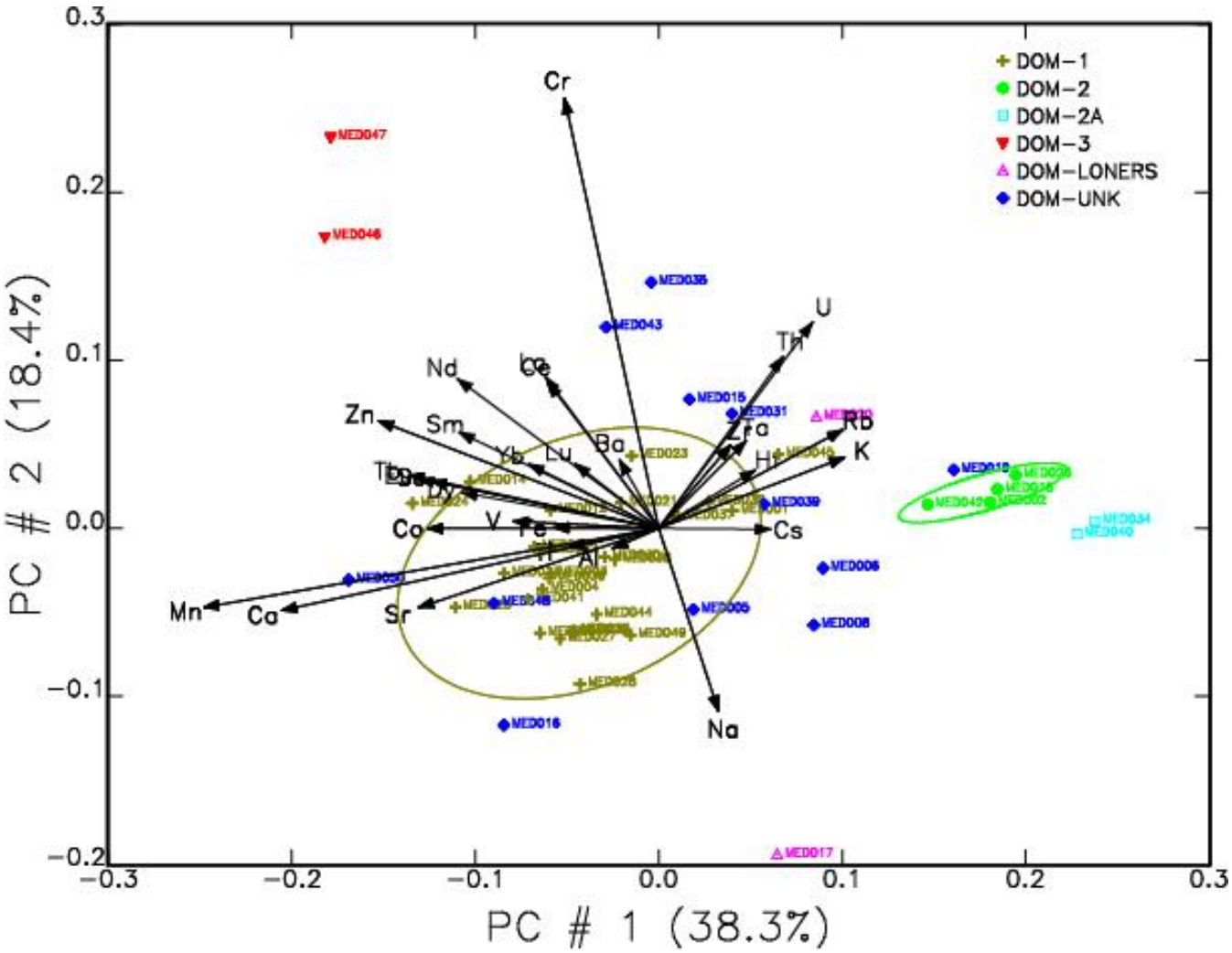

Figure 1: Principal component biplot of first two components (56.7% total variance) showing clays and ceramic samples. Elemental loading vectors are shown and labeled.

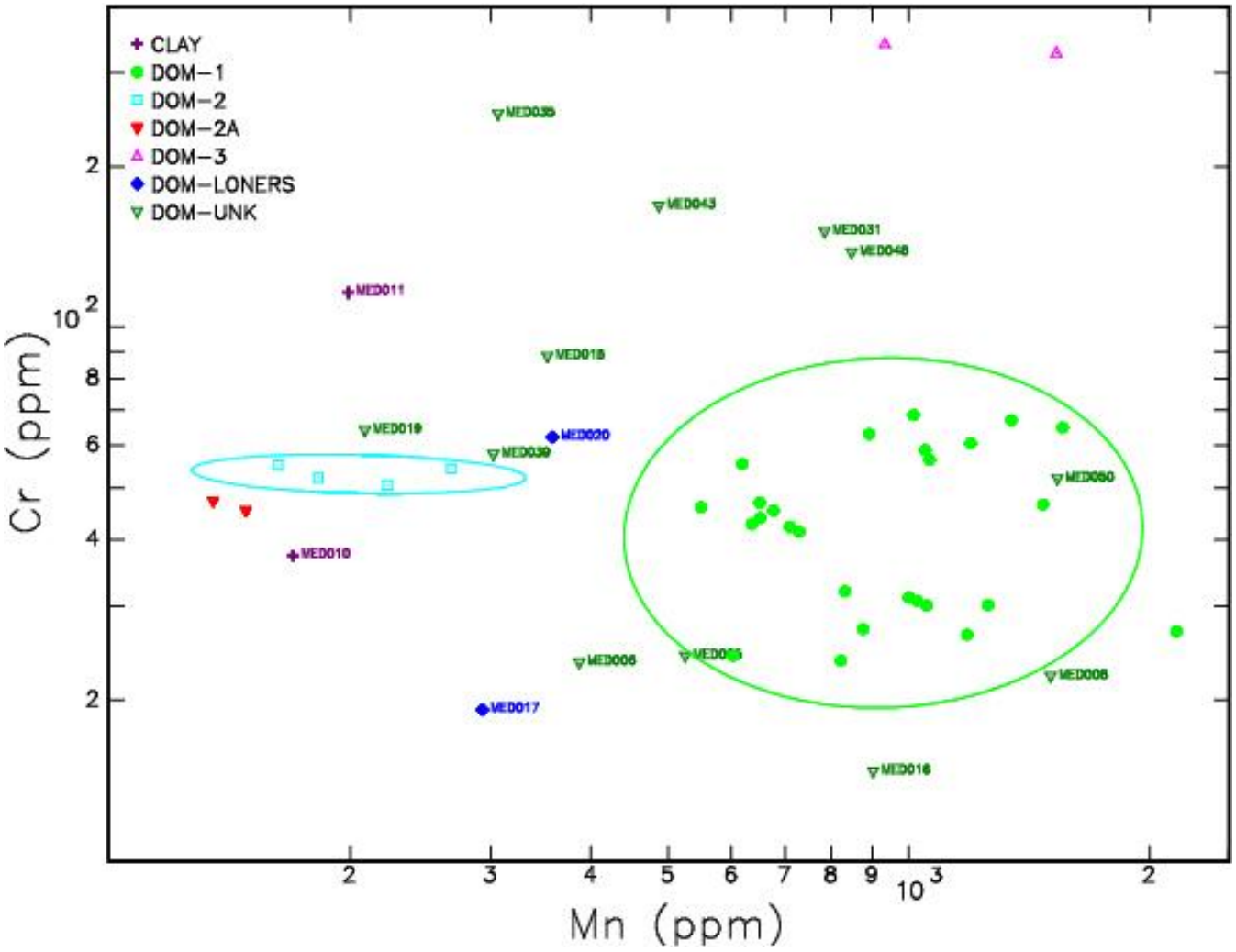

Figure 2: Bivariate plot comparing Manganese (Mn) and Chromium (Cr) concentrations (ppm). Ellipses are drawn at the 90% confidence interval.

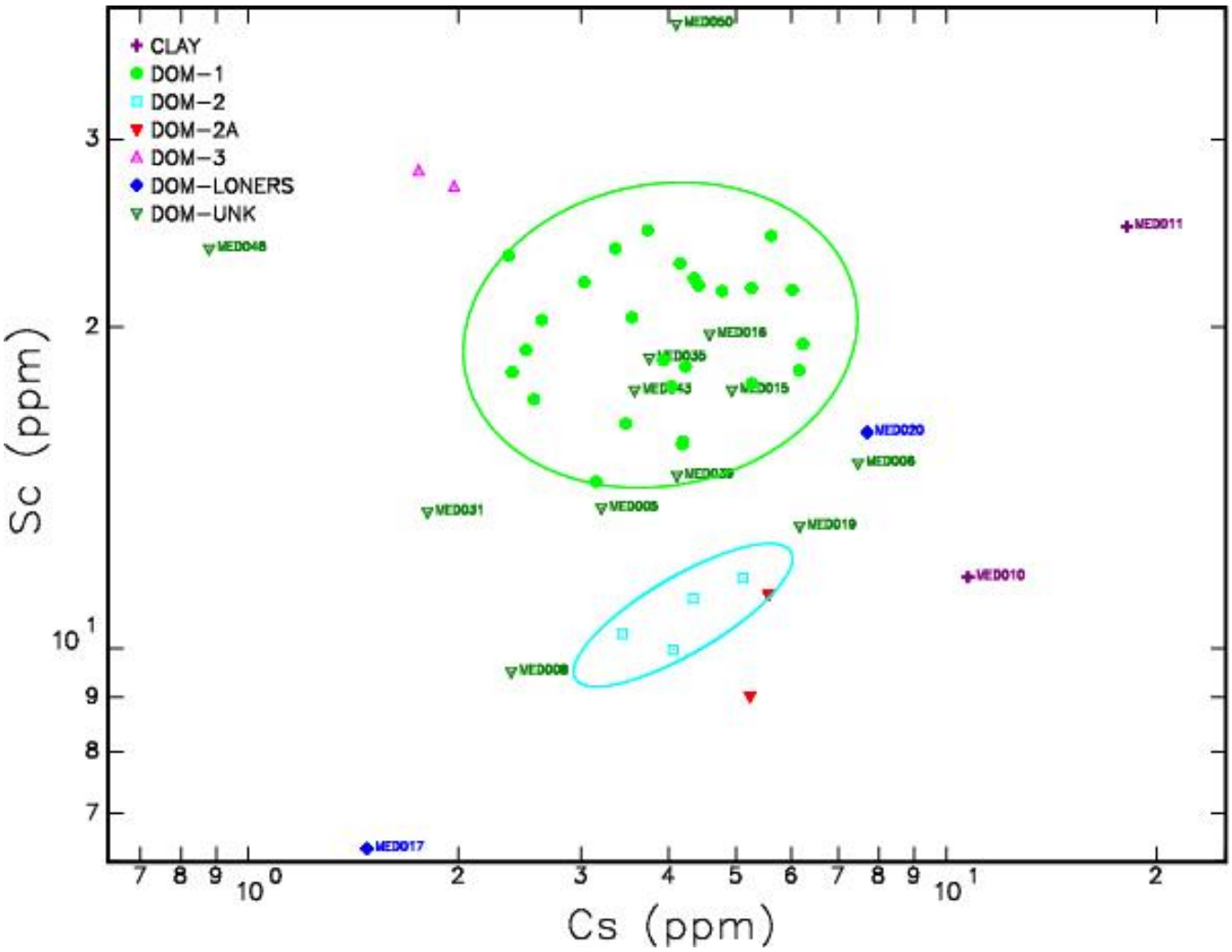

Figure 2: Bivariate plot comparing Cesium (Cs) and Scandium (Sc) concentrations (ppm). Ellipses are drawn at the 90% confidence interval.

Table 2: Mahalanobis distance–based probabilities (*p*) of group membership for DOM-1. * denotes DOM-1 associated members. Mahalanobis distances calculated using first ten PCs (94.4% total variance).

DOM-1	*p*	Clay	*p*	DOM-2	*p*	DOM-2A	*p*	DOM-2	*p*	DOM-UNK	*p*
MED001	1.57	MED010	0.00	MED002	0.11	MED034	0.01	MED046	0.00	MED005	0.05
MED003	96.52	MED011	0.31	MED018	0.85	MED040	0.00	MED047	0.00	MED006	0.22
MED004	49.63			MED026	0.03					MED008	0.21
MED007	21.03			MED042	0.26					MED015	2.57
MED009	88.01									MED016*	18.41
MED012	7.32									MED019	0.15
MED013	37.04									MED031	0.00
MED014	26.82									MED035	0.01
MED021	43.36									MED039	0.72
MED022	70.83									MED043	0.12
MED023	76.05									MED048	0.00
MED024	15.24									MED050	0.79
MED025	75.37										
MED027	99.49										
MED028	16.96										
MED029	42.10										
MED030	93.32										
MED032	4.18										
MED033	15.23										
MED036	82.92										
MED037	63.83										
MED038	96.60										
MED041	52.99										
MED044	89.62										
MED045	4.70										
MED049	25.17										

Appendix II: Total Variation Matrix

	Na	Al	K	Ca	Sc	Ti	V	Cr	Mn	Fe	Co	Zn	Rb	Sr	Zr
Na	0	0.157	0.258	0.409	0.368	0.247	0.298	0.852	0.735	0.254	0.376	0.5	0.316	0.301	0.289
Al	0.157	0	0.181	0.272	0.117	0.054	0.098	0.502	0.449	0.067	0.132	0.186	0.198	0.222	0.115
K	0.258	0.181	0	0.681	0.4	0.269	0.326	0.613	0.828	0.282	0.404	0.497	0.046	0.565	0.115
Ca	0.409	0.272	0.681	0	0.199	0.262	0.236	0.718	0.33	0.265	0.182	0.247	0.695	0.141	0.482
Sc	0.368	0.117	0.4	0.199	0	0.084	0.066	0.473	0.311	0.06	0.054	0.089	0.354	0.318	0.219
Ti	0.247	0.054	0.269	0.262	0.084	0	0.025	0.536	0.384	0.02	0.077	0.186	0.243	0.281	0.112
V	0.298	0.098	0.326	0.236	0.066	0.025	0	0.491	0.352	0.016	0.062	0.173	0.291	0.299	0.167
Cr	0.852	0.502	0.613	0.718	0.473	0.536	0.491	0	1.01	0.487	0.558	0.483	0.582	0.688	0.469
Mn	0.735	0.449	0.828	0.33	0.311	0.384	0.352	1.01	0	0.379	0.243	0.387	0.836	0.563	0.612
Fe	0.254	0.067	0.282	0.265	0.06	0.02	0.016	0.487	0.379	0	0.071	0.157	0.239	0.307	0.137
Co	0.376	0.132	0.404	0.182	0.054	0.077	0.062	0.558	0.243	0.071	0	0.155	0.368	0.311	0.217
Zn	0.5	0.186	0.497	0.247	0.089	0.186	0.173	0.483	0.387	0.157	0.155	0	0.442	0.328	0.328
Rb	0.316	0.198	0.046	0.695	0.354	0.243	0.291	0.582	0.836	0.239	0.368	0.442	0	0.629	0.11
Sr	0.301	0.222	0.565	0.141	0.318	0.281	0.299	0.688	0.563	0.307	0.311	0.328	0.629	0	0.448
Zr	0.289	0.115	0.115	0.482	0.219	0.112	0.167	0.469	0.612	0.137	0.217	0.328	0.11	0.448	0
Cs	0.382	0.245	0.288	0.691	0.309	0.22	0.266	0.808	0.833	0.205	0.326	0.389	0.161	0.673	0.225
Ba	0.371	0.172	0.284	0.515	0.267	0.209	0.248	0.622	0.666	0.219	0.299	0.296	0.264	0.354	0.266
La	0.348	0.118	0.257	0.313	0.133	0.145	0.169	0.366	0.526	0.151	0.186	0.144	0.246	0.307	0.155
Ce	0.37	0.107	0.248	0.314	0.116	0.13	0.157	0.372	0.481	0.138	0.165	0.148	0.231	0.33	0.134
Nd	0.483	0.161	0.399	0.307	0.119	0.154	0.163	0.409	0.458	0.163	0.175	0.157	0.393	0.33	0.231
Sm	0.359	0.106	0.318	0.228	0.064	0.119	0.134	0.45	0.371	0.126	0.127	0.11	0.322	0.278	0.185
Eu	0.327	0.098	0.371	0.151	0.074	0.124	0.137	0.486	0.338	0.139	0.122	0.111	0.392	0.186	0.233
Tb	0.422	0.19	0.449	0.261	0.066	0.167	0.162	0.604	0.358	0.162	0.134	0.141	0.423	0.384	0.261
Dy	0.333	0.113	0.331	0.253	0.061	0.117	0.136	0.574	0.321	0.126	0.122	0.156	0.336	0.329	0.199
Yb	0.33	0.128	0.274	0.326	0.075	0.127	0.147	0.545	0.404	0.13	0.142	0.192	0.267	0.411	0.153
Lu	0.326	0.142	0.239	0.395	0.097	0.136	0.16	0.571	0.444	0.137	0.154	0.233	0.217	0.484	0.143
Hf	0.259	0.106	0.105	0.496	0.235	0.108	0.173	0.521	0.645	0.138	0.244	0.331	0.087	0.449	0.022
Ta	0.274	0.1	0.132	0.506	0.215	0.095	0.155	0.449	0.664	0.118	0.235	0.301	0.091	0.438	0.042
Th	0.374	0.193	0.134	0.625	0.314	0.196	0.244	0.416	0.809	0.213	0.338	0.399	0.109	0.544	0.067
U	0.482	0.274	0.17	0.741	0.465	0.319	0.391	0.439	0.956	0.365	0.466	0.541	0.203	0.564	0.151
$\tau_{.i}$	10.801	5.001	9.467	11.239	5.723	5.145	5.742	16.093	15.694	5.273	6.446	7.806	9.089	11.461	6.287
$vt/\tau_{.i}$	0.362	0.782	0.413	0.348	0.683	0.76	0.681	0.243	0.249	0.742	0.607	0.501	0.43	0.341	0.622
$r.v\tau.$	0.586	0.938	0.516	0.371	0.789	0.935	0.875	0.251	0.332	0.916	0.736	0.69	0.534	0.394	0.738

	Cs	Ba	La	Ce	Nd	Sm	Eu	Tb	Dy	Yb	Lu	Hf	Ta	Th	U
Na	0.382	0.371	0.348	0.37	0.483	0.359	0.327	0.422	0.333	0.33	0.326	0.259	0.274	0.374	0.482
Al	0.245	0.172	0.118	0.107	0.161	0.106	0.098	0.19	0.113	0.128	0.142	0.106	0.1	0.193	0.274
K	0.288	0.284	0.257	0.248	0.399	0.318	0.371	0.449	0.331	0.274	0.239	0.105	0.132	0.134	0.17
Ca	0.691	0.515	0.313	0.314	0.307	0.228	0.151	0.261	0.253	0.326	0.395	0.496	0.506	0.625	0.741
Sc	0.309	0.267	0.133	0.116	0.119	0.064	0.074	0.066	0.061	0.075	0.097	0.235	0.215	0.314	0.465
Ti	0.22	0.209	0.145	0.13	0.154	0.119	0.124	0.167	0.117	0.127	0.136	0.108	0.095	0.196	0.319
V	0.266	0.248	0.169	0.157	0.163	0.134	0.137	0.162	0.136	0.147	0.16	0.173	0.155	0.244	0.391
Cr	0.808	0.622	0.366	0.372	0.409	0.45	0.486	0.604	0.574	0.545	0.571	0.521	0.449	0.416	0.439
Mn	0.833	0.666	0.526	0.481	0.458	0.371	0.338	0.358	0.321	0.404	0.444	0.645	0.664	0.809	0.956
Fe	0.205	0.219	0.151	0.138	0.163	0.126	0.139	0.162	0.126	0.13	0.137	0.138	0.118	0.213	0.365
Co	0.326	0.299	0.186	0.165	0.175	0.127	0.122	0.134	0.122	0.142	0.154	0.244	0.235	0.338	0.466
Zn	0.389	0.296	0.144	0.148	0.157	0.11	0.111	0.141	0.156	0.192	0.233	0.331	0.301	0.399	0.541
Rb	0.161	0.264	0.246	0.231	0.393	0.322	0.392	0.423	0.336	0.267	0.217	0.087	0.091	0.109	0.203
Sr	0.673	0.354	0.307	0.33	0.33	0.278	0.186	0.384	0.329	0.411	0.484	0.449	0.438	0.544	0.564
Zr	0.225	0.266	0.155	0.134	0.231	0.185	0.233	0.261	0.199	0.153	0.143	0.022	0.042	0.067	0.151
Cs	0	0.291	0.339	0.325	0.449	0.375	0.435	0.372	0.358	0.305	0.261	0.188	0.155	0.248	0.456
Ba	0.291	0	0.179	0.184	0.237	0.197	0.214	0.306	0.233	0.26	0.252	0.247	0.189	0.27	0.347

La	0.339	0.179	0	0.013	0.076	0.051	0.076	0.153	0.112	0.105	0.128	0.161	0.134	0.15	0.246
Ce	0.325	0.184	0.013	0	0.077	0.045	0.076	0.146	0.099	0.097	0.116	0.141	0.121	0.148	0.245
Nd	0.449	0.237	0.076	0.077	0	0.053	0.079	0.146	0.104	0.118	0.161	0.24	0.215	0.274	0.359
Sm	0.375	0.197	0.051	0.045	0.053	0	0.019	0.06	0.023	0.045	0.082	0.196	0.179	0.248	0.349
Eu	0.435	0.214	0.076	0.076	0.079	0.019	0	0.08	0.043	0.088	0.136	0.248	0.232	0.313	0.392
Tb	0.372	0.306	0.153	0.146	0.146	0.06	0.08	0	0.048	0.072	0.102	0.287	0.271	0.372	0.529
Dy	0.358	0.233	0.112	0.099	0.104	0.023	0.043	0.048	0	0.022	0.048	0.207	0.2	0.293	0.413
Yb	0.305	0.26	0.105	0.097	0.118	0.045	0.088	0.072	0.022	0	0.015	0.162	0.16	0.224	0.354
Lu	0.261	0.252	0.128	0.116	0.161	0.082	0.136	0.102	0.048	0.015	0	0.144	0.143	0.211	0.339
Hf	0.188	0.247	0.161	0.141	0.24	0.196	0.248	0.287	0.207	0.162	0.144	0	0.022	0.061	0.168
Ta	0.155	0.189	0.134	0.121	0.215	0.179	0.232	0.271	0.2	0.16	0.143	0.022	0	0.056	0.172
Th	0.248	0.27	0.15	0.148	0.274	0.248	0.313	0.372	0.293	0.224	0.211	0.061	0.056	0	0.12
U	0.456	0.347	0.246	0.245	0.359	0.349	0.392	0.529	0.413	0.354	0.339	0.168	0.172	0.12	0
$\tau_{.i}$	10.576	8.457	5.485	5.274	6.688	5.22	5.72	7.127	5.708	5.678	6.015	6.392	6.061	7.965	11.014
$vt/\tau_{.i}$	0.37	0.462	0.713	0.742	0.585	0.749	0.684	0.549	0.685	0.689	0.65	0.612	0.645	0.491	0.355
$r.v\tau.$	0.673	0.818	0.904	0.922	0.827	0.864	0.752	0.78	0.855	0.926	0.921	0.72	0.731	0.591	0.448
vτ	3.911														